

# Segmentation and Reconstruction of the Pulmonary Parenchyma

Aristófanés C. Silva<sup>1\*</sup>, Paulo Cezar P. Carvalho<sup>2</sup>, Rodolfo A. Nunes<sup>3</sup>

<sup>1\*</sup> *Pontifical Catholic University of Rio de Janeiro - PUC-Rio, Rua Marquês de São Vicente, 225, Gávea - 22453-900  
Rio de Janeiro-RJ, Brazil*

*Federal University of Maranhão - UFMA, Av. dos Portugueses, s/n, 65085-580 São Luís-MA, Brazil*  
*Corresponding author : e-mail: ari@visgraf.impa.br; Tel: +55-21-25295080; fax: +55-21-25295067*

<sup>2</sup> *Institute of Pure and Applied Mathematics - IMPA, Estrada D. Castorina, 110, 22460-320 Rio de Janeiro-RJ, Brazil*  
*e-mail: pcezar@impa.br*

<sup>3</sup> *State University of Rio de Janeiro - UERJ, Av. 28 de Setembro, 87, 22460-320 Rio de Janeiro-RJ, Brazil*  
*e-mail: rodolfo@solt.com.br*

# Segmentation and Reconstruction of the Pulmonary Parenchyma

## Abstract

This work presents a method for the segmentation and reconstruction of the pulmonary parenchyma in CT images. The identification and outline of the pulmonary parenchyma is essential to analyze the pulmonary volume and is an important stage in automatic or semi-automatic processes for detecting lesions, vessels and the bronchial tree.

The method proposed here combines traditional concepts, such as global-threshold segmentation, mathematical morphology, border detection and chain code, with new ideas, such as area classification of pulmonary structures and border reconstruction, when the lesion is adjacent to the pleura.

We performed tests with 150 computed-tomography images and observed that 135 of them provided good results.

Keywords: segmentation, border segmentation, border detection, pulmonary parenchyma, pulmonary region.

## 1 Introduction

Lung cancer is the most common of all visceral malign tumors, presenting an yearly increase of 2% in its global incidence. In Brazil, lung cancer was expected to affect 20,835 people, being 14,900 men and 5,935 women, causing 15,145 deaths in 2001 [7]. This is the type of cancer that causes the largest number of deaths. Nevertheless, it is a fact that, the sooner the lesion is detected, the greater is patient survival. There have been stimulating technology improvements, such as helical tomography and, more recently, multislice tomography. New computational methods have also been developed to aid doctors in lesion detection and diagnosis.

Though the lung composition provides a natural radiological contrast, there are some difficulties in the identification and diagnosis of lesions, which derive from the fact that the lung has anatomic structures with similar characteristics (shapes, densities, etc.). For certain lesions, especially for small ones, computer-aided resources have been developed to help specialists in this task. Among such tools, automatic enhancement, segmentation and classification algorithms are being studied. In segmentation, the initial step - pulmonary parenchyma segmentation - is extremely important. By extracting the pulmonary parenchyma, the area to be segmented is restricted, eliminating structures that add difficulty to the process, such as vessels, bronchi, the thoracic wall and the mediastinum.

In the present article, we will describe an automatic segmentation method for the pulmonary parenchyma. The method is based on a combination of traditional techniques, such as segmentation using global threshold, morphological opening and closing operations, border detection using Sobel's filter, thinning, representation of pulmonary structures using chain code, classification of the structures' areas and reconstruction of the pulmonary parenchyma using rolling-ball algorithm.

Section 2 discusses the importance of extracting the pulmonary area for automatic algorithms that detect the lung's internal structure, mentioning some existing works on the subject. In Section 3, the equipment and the acquisition conditions of exams are described. In Section 4, the method resulting from our research is proposed, its details are analyzed and the obtained results are presented.

## 2 Related Work

The idea of segmenting the pulmonary parenchyma before executing any other automatic segmentation specific for lesions is not new. In fact, it is an almost obligatory step.

Reeves and Kostis [12] summarize several attempts to perform computer-aided diagnosis. They have classified the methods in three stages: identification of the pulmonary area, separation of supposed nodules from the vessels, and classification of the nodules. They also emphasize that the first stage is the most important.

Before segmenting pathological pulmonary regions using Lymphagioliomyomatosis (LAM), Everhart [4] segments the lungs using global threshold and region-growing techniques.

Tesuya et al [13] segment the pulmonary parenchyma using global threshold and, subsequently, the expansion-contraction algorithm, since lungs are composed almost completely by air, thus having a much lower density than bone and fat.

To segment separate nodules, Stephan et al [3] needed to extract the pulmonary parenchyma first, in order to avoid problems in their segmentation.

In the work by Bohm et al [10], whose purpose was to segment the bronchial tree, firstly the pulmonary parenchyma was extracted using the region-growing algorithm (threshold = -400 HU), combining morphological operations to include high-density structures inside the parenchyma.

Kanazawa et al [9] developed an automatic detection system for pulmonary nodules using several tools, such as thresholds, the fuzzy clustering method, metric tools (area, perimeter, circularity, etc.) and contrast. The first step of such system is the extraction of the pulmonary parenchyma.

## 3 Methods and Equipment

To test the proposed method, we used color images acquired from GE Pro Speed helical tomography under the following conditions: voltage of the tube of 120 Kv, current of the tube of 100 mA, 512x512 image size and 2 mm reconstruction interval.

The images were quantized in 12 bits and stored in DICOM format. In the present work, we used 150 tomography images from several patients with pulmonary nodules. Figure 1 shows an example of an image used for the tests.

The proposed method was applied to each slice of each patient's exam, and the final results of the segmentation were evaluated by medical doctors. The method was implemented in C++, using two additional libraries for interface and drawing - IUP [11] and CD [1], respectively, developed by the Tecgraf laboratory - and compiled with Microsoft's Visual C++.

## 4 Segmentation

The sequence of steps for our method is shown in Figure 2. The threshold step produces a binary image that provides a rough version of the pulmonary parenchyma. With the closing and opening proceedings, small structures contained in the pulmonary parenchyma are eliminated and some breaches in the borders are corrected. Border detection and thinning have the purpose, respectively, of extracting the structure's borders and thinning them to the width of a pixel. Finally, the object-extraction step seeks to eliminate all uninteresting objects, leaving only the pulmonary parenchyma. In some images, the nodule is adjacent to the pleura, which causes the result provided by the previous steps to be incorrect. For these cases, a new step was added to reconstruct the border breach caused by the nodule.

In the subsections below we describe, in detail, each one of the segmentation steps and we show the results of applying these steps to the image in Figure 1.



Figure 1: Original CT showing a pulmonary nodule to the left.

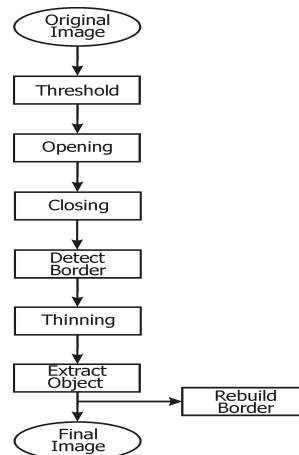


Figure 2: Structure of the segmentation and reconstruction method.

#### 4.1 Global Threshold

The first step of the method is to segment each slice of the computed tomography (CT) to detach the lung from the thoracic wall, the mediastinum and other structures. The slices are segmented with a global threshold of -250 HU (Hounsfield Unit) [4], because the lung is filled mainly by air. The application of Equation 1 generates a binary image:

$$g(i, j) = \begin{cases} 1, & \text{if } f(i, j) \geq -250HU \\ 0, & \text{if } f(i, j) < -250HU \end{cases} \quad (1)$$

Observing the image resulting from the threshold, presented in Figure 3, one can note that the image background has the same density as the lung. There are also some main airway structures from the windpipe bifurcation that can make the extraction of the pulmonary parenchyma more difficult. Therefore, there is the need to apply additional proceedings to complete the extraction of the pulmonary region.

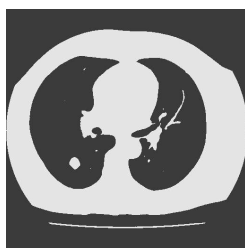


Figure 3: Segmented CT with threshold -250 HU, showing bronchial structures.

## 4.2 Opening and Closing

The basic principle of mathematical morphology [2, 6, 8] consists in extracting information relative to the geometry and topology of a well defined set, called structuring element. Mathematical morphology has two basic operations: dilation and erosion.

The dilation operation causes the effect of increasing the size of the object, and it is defined by:

$$A \oplus B = \{c | c = a + b, a \in A, b \in B\} \quad (2)$$

The erosion operation has the effect of diminishing the size of the object. It is expressed by:

$$A \ominus B = \{c | (B)_c \subseteq A\} \quad (3)$$

In Equations 2 and 3,  $A$  represents the image to which the operation is applied and  $B$  is the structuring element.

Two other operations – opening and closing – derive from the dilatation and erosion operations.

The opening operation generally smoothes the outline of an image and breaks narrow isthmuses and thin prominences. It is given by:

$$A \circ B = (A \ominus B) \oplus B \quad (4)$$

In our method, the opening operation aims at eliminating small and usually thin objects inside the lung, and at separating some regions that make the identification of the lung border more difficult.

On the other hand, the closing operation unites small breaches, widens narrow gulfs, eliminates small orifices and fills border interruptions. It can be expressed by:

$$A \bullet B = (A \oplus B) \ominus B \quad (5)$$

In our method, the closing operation has the purpose of improving border definition, filling holes in the border that caused interruptions when the border-detection algorithm was applied. Such interruptions bring difficulties to the object-removal step, that follows border detection, which examines the border to determine whether the object is closed.

Empirically, we verified that the best results were obtained when the opening operation was applied three times followed by two applications of the closing operation, both with a  $3 \times 3$  structure element.

Figure 4 shows the result of applying these two operations, in the manner described above, to the image in Figure 1.



Figure 4: Three opening and two closing operations applied to the image.

### 4.3 Border Detection

Detecting the image border is an essential step to process the rest of the algorithm. In this step, the borders are thinned and highlighted. We use Sobel's operator [2, 6, 8], with the following mask:

$$\begin{bmatrix} -1 & -2 & 1 \\ 0 & 0 & 0 \\ 1 & 2 & 1 \end{bmatrix} \begin{bmatrix} -1 & 0 & 1 \\ -2 & 0 & 2 \\ -1 & 0 & 1 \end{bmatrix}$$

This operator is robust enough for this type of image, since there is no need to detect vertical or horizontal lines. Figure 5 shows the application of Sobel's operator to the CT image in Figure 4.

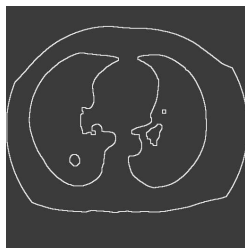


Figure 5: Border-detection operation applied to the image.

### 4.4 Thinning

The main purpose of the image-thinning operation is to create a compact representation of the desired structure. However, this operation is highly sensitive to noise, small irregularities or interruptions. For this step of our method, we used the Zhang and Suen algorithm [2, 6, 8], which reduces the borders, detected in the previous step, to the width of one pixel. The result of this operation is presented in Figure 6.

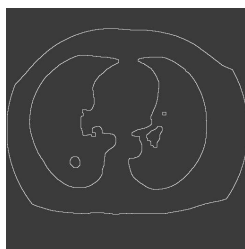


Figure 6: Thinning operation applied to the image.

### 4.5 Object Removal

As can be seen in Figure 6, there remain in the image structures, other than the lungs, which are not interesting for the algorithm. This step removes such structures, leaving only the pulmonary parenchyma.

First, the whole image is examined, and, using chain code representation [2, 6, 8], we can determine the initial and final coordinates and compute the area of each object in the image.

Three criteria were adopted to remove uninteresting objects:

1. Small length of the object's border

Objects with border length smaller than or equal to 300 pixels are eliminated. To save space in the storing vector and in subsequent proceedings, objects that satisfy this condition are immediately eliminated.

2. Non-closed objects

Objects that are not closed are eliminated. Based on the created data structure, we can simply check if the final coordinates are the same as the initial coordinates.

3. Area classification

As one can observe in the image, the largest areas, in decreasing order, are: thoracic wall, right and left lungs and, following, other internal lung structures, such as nodules, vessels, etc. (see Figure 7). With such information, we can sort the data structure according to the objects in the image, in decreasing order. The largest structure is discarded (since it should correspond to the thoracic wall). The next two objects correspond to the left and the right lungs, respectively, and are saved. All remaining objects are discarded.

Figure 8 shows the resulting image after this step. The steps above are described in the algorithm 1

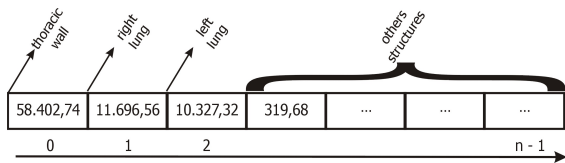


Figure 7: Data structure classified by area in  $mm^2$

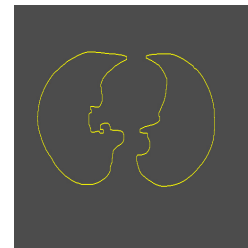


Figure 8: Image after the removal of uninteresting objects.

## 4.6 Results

By applying the algorithm described in the previous sections, we have obtained the image shown in Figure 9. Figure 10 presents the 3D visualization of a series of 26 slices that contains the slice in Figure 9.

## 4.7 Reconstructing the Pulmonary Parenchyma

In some cases, the pulmonary lesion is adjacent to the pleura and has similar densities. Therefore, when the first step - global threshold - of our method is processed, concave depressions appear on

---

**Algorithm 1** Object Removal

---

```
1: for  $z = 0$  to  $L - 1$  do { $n$  slices}
2:   Initialize array with zeros
3:   for  $i = 0$  to  $N - 1$  do {rows}
4:     for  $j = 0$  to  $M - 1$  do {columns}
5:       ChainCode() {return  $n$  (size of chain)}
6:       if  $n > \text{LIMCHAIN}$  then {LIMCHAIN = 200, in order to remove small objects}
7:          $area = \text{CalculeArea}()$ 
8:         Store area in array
9:       end if
10:    end for
11:  end for
12:  for  $k = 0$  to  $sizearray$  do {remove object of array}
13:    if  $Object[k].Xi \neq Object[k].Xf$  and  $Object[k].Yi \neq Object[k].Yf$  then
14:      delete object {opened object}
15:    end if
16:  end for
17:  Sorting array
18:  Select and set only Object[1] and Object[2] {right and left lung}
19: end for
```

---

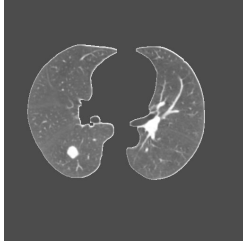


Figure 9: CT after all steps were applied.

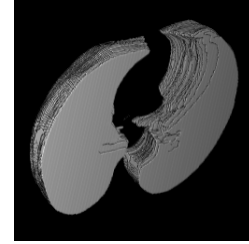


Figure 10: 3D visualization of 26 CT slices.

the lesion location. For the correct extraction of the pulmonary parenchyma, this depression must be rebuilt. Figure 11 shows an image with a nodule adjacent to the pleura, and Figure 12 presents the depression resulting from applying the previously describe steps.

The technique used to reconstruct the pulmonary parenchyma is the rolling-ball operator [5], that fills out the depression employing a morphological operation that uses a disk as structuring element. The operator is defined by:

$$g = (A \bullet B) - A \quad (6)$$

where  $A$  is the segmented image,  $B$  is the structuring element and  $g$  is the resulting image.

The user defines the radius of the disk and the area where the rolling-ball should act. If this area





Figure 11: Image with a nodule adjacent to the pleura.

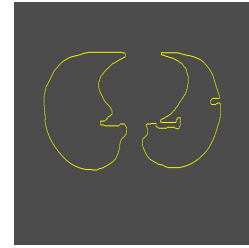


Figure 12: Image with depression on the thoracic wall.

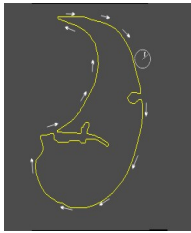


Figure 13: Rolling-ball technique.

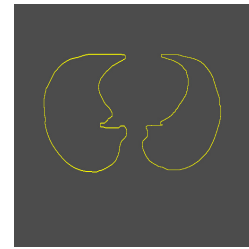


Figure 14: Image with rebuilt thoracic wall.

is not specified, the operation is applied to the entire image.

The Figure 13 illustrates the rolling-ball technique and the Figures 14 and 15 show the result of the pulmonary parenchyma reconstruction algorithm.

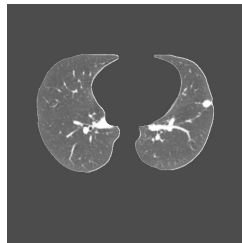


Figure 15: Image with rebuilt thoracic wall reinserted in the original image.

## 5 Analysis of the Results

The tests for the method were done with 7 exams, which generated 150 CT images.

After performing the tests, we observed that in 135 images the results matched our expectation, that is, the method correctly extracted and reconstructed the pulmonary parenchyma.

In the other 15 images, the results were incorrect. This is due to the anatomic characteristics

of one patient's lungs, as can be seen in Figure 16. This patient had a nodular lesion with a very irregular and spiculated shape, located at the top of the right lung and having some contact with the pleura. The step of the method that caused the error was the application of opening and closing morphological operators, which was unable to separate the lungs from the windpipe. This turned the windpipe and the lungs into only one object, which became the second largest object after the thoracic wall. The nodule, on its turn, was considered the third largest object in the classification of the lung's internal structures, being accepted as a structure of interest. The incorrect result of the segmentation is presented in Figure 17. This problem can be solved by applying Hough's transform to detect the windpipe and separate both lungs, as described by Everhart et al [4].

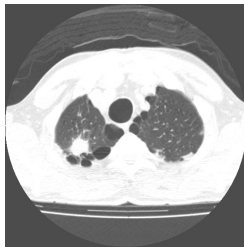


Figure 16: Image that caused the segmentation error.

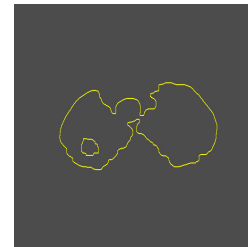


Figure 17: Incorrectly segmented image.

## 6 Conclusion

A method to segment and reconstruct the pulmonary parenchyma was presented. The segmentation is based on a sequence of simple and traditional operations, such as global-threshold segmentation, opening and closing, border detection, thinning, chain code, and classification of the structures area. The reconstruction of the pulmonary parenchyma, necessary when the nodule is adjacent to the pleura, is based on the rolling-ball operator.

With such operations, we have reached the proposed objective and obtained good results, which stimulate us to continue on our research. However, since our future goal is to build a complete tool to support diagnoses of pulmonary nodules, we believe there is a need for an automatic or semi-automatic nodule-segmentation method in 2D and 3D to better evaluate volume modifications in time and to promote the detachment and distinction of vascular structures, thus performing a

more detailed analysis and classification of internal nodule structures – for instance, into areas of calcification, necrosis and fibrosis.

## 7 Acknowledgements

We would like to thank CAPES and FAPERJ for the financial support.

We also thank Gustavo Adolpho Moreira Faulhaber, Fabrízia Rennó Soderó, Patrícia Damasco and Jonas Araújo de Souza for the medical support, and the staff of Instituto Fernandes Figueira, especially Dr. Márcia Cristina Bastos Boechat, for the images provided.

## References

- [1] Canvas Draw CD (2001). Grupo de Tecnologia Gráfica TecGraf. Available at: [<http://www.tecgraf.puc-rio.br/cd>]. Accessed August 21, 2001.
- [2] Castleman KR (1996), Digital Image Processing. Prentice Hall, Englewood Cliffs, NJ, USA.
- [3] Erberich SG, Song KS, Arakawa H, Huang HK, Webb R, Hoo KS, Loo BW (1999), Knowledge-Based Lung Nodule Detection from Helical CT. *Bildverarbeitung für die Medizin*, pp 337-341.
- [4] Everhart J, Cannon M, Newell J, Lynch D (1994), Image Segmentation Applied to CT Examination of Lymphangiomyomatosis (LAM). *SPIE Medical Imaging 1994: Image Processing*, 2167:87-95.
- [5] Facon J (1996), *Morfologia Matemática : Teoria e Exemplos*. Editora Universitária Católica do Paraná, Curitiba, Brazil.
- [6] Gonzalez RC, Woods RE (1992), *Digital Image Processing*, 3rd edition, Addison-Wesley, Reading, MA, USA.
- [7] Instituto Nacional do Câncer-INCA (2001), Câncer de Pulmão. Available at: [<http://www.inca.org.br/cancer/tipos/pulmao.html>], Accessed August 08, 2001.
- [8] Jain AK (1989), *Fundamentals of Digital Image Processing*. Prentice Hall, Englewood Cliffs, NJ, USA.
- [9] Kanazawa K, Kawata Y, Niki N, Satoh H, Ohmatsu H, Kakinuma R, Kaneko M, Moriyama N, Eguchi K (1998), Computer-aided diagnosis for pulmonary nodules based on helical CT images. *Computerized Medical Imaging and Graphics*, 22:157-167.
- [10] Krass S, Selle D, Boehm D, Peitgen O, Bremen H, Jend H, Kriete A, Rau W (2000), Determination of bronchopulmonary segments based on HRCT data. *Computer Assisted Radiology and Surgery*, 584-589
- [11] Levy C, Gattass M, Lucena C (1996), IUP : A Portable User Interface Development Tool. *Software: Practice and Experience*, 267:737-762.

- [12] Reeves AP, Kostis WJ (2000), Computer-Aided Diagnosis for Lung Cancer. *Radiologic Clinics of North America*, 38:1-11
- [13] Tozak T, Kawata Y, Ohmatsu H, Eguchi K, Moriyama N, (1996), Three-Dimensional Analysis of Lung Areas Using Thin Slice CT Images. In: Hoffman EA, *Physiology and Function from Multidimensional Images*, Newport Beach, CA, USA, pp 2-11.